Stability analysis for extended models of gap solitary waves

J. Schöllmann and A. P. Mayer
Institut für Theoretische Physik, Universität Regensburg, D-93040 Regensburg, Germany
(Received 13 September 1999)

A numerical linear stability analysis has been carried out for stationary spatially localized solutions of several systems of coupled nonlinear partial differential equations (PDE's) with two and more complex variables. These coupled PDE's have recently been discussed in the literature, mostly in the context of physical systems with a frequency gap in the dispersion relation of their linear excitations, and they are extensions of the Mills-Trullinger gap soliton model. Translational and oscillatory instabilities are identified, and their associated growth rates are computed as functions of certain parameters characterizing the solitary waves.

PACS number(s): 42.65.Tg, 42.81.Dp, 42.70.Qs, 42.65.Sf

I. INTRODUCTION

In nonlinear physical systems that have frequency gaps in the dispersion relation of their linear excitations, there can be stationary or slowly moving nonlinear modes that are spatially localized and have frequencies outside the frequency bands of the linear modes. Band gaps can be generated by periodic modulations of continuous physical systems or by discreteness. Such nonlinear modes have been discussed in various physical contexts in both discrete and continuous systems, and in particular in nonlinear optics. Interest in these gap solitary waves has been strongly enhanced by recent experiments on Bragg grating fibers by Eggleton *et al.* [1], and by the fabrication of optical band-gap materials [2]. For the latter, stationary gap solitary waves have been predicted in two and three dimensions [3].

If the effects of periodic modulation and nonlinearity are of the same order of magnitude, gap solitary waves emerge as solutions of a system of coupled partial differential equations (PDE's) for the complex amplitudes of plane or guided waves with wave vectors at the boundary of the Brillouin zone corresponding to the dispersion relation of the linear modes of the physical system. In the one-dimensional case, to which we shall confine our discussion here, and for third-order nonlinearity, analytical solutions of the corresponding PDE's are known for stationary [4] and moving [5,6] solitary waves. In the following, we shall call these PDE's Mills-Trullinger (MT) equations. In field theory, PDE's of this type have been studied earlier, and solitary wave solutions had been found in one and higher dimensions (see the corresponding references in Ref. [7]). The massive Thirring model [8] constitutes an integrable limiting case of the MT equations [9].

Various extensions and modifications of these equations have also been studied, including resonant coupling of the waves at the Brillouin-zone boundary with their second harmonic [10–16], three-wave mixing [17], coupling to a diffusive degree of freedom [16], additional dispersion terms [18], and the effect of optical rectification [19].

Although solitary wave solutions of these equations have been partially known for a long time, a systematic analysis of their stability by linearizing the PDE's with respect to deviations from the solitary wave solutions was carried out only recently [20,21,16,7,3]. For the MT equations and the PDE's describing resonant coupling between fundamental zone-boundary modes and their second harmonics, this analysis has revealed that the gap solitary waves are stable in certain regions of parameter space, while in others, the dominant role in the instability found here is played by complex eigenvalues of the corresponding linearized system [20,16,7]. These eigenvalues have imaginary parts (frequencies) much larger than their real parts (growth rates), and their associated eigenvectors are normally extended far beyond the spatial extension of the solitary wave. This type of instability was found earlier in continuous systems [22,23] and a discrete system [24], and has been termed an *oscillatory instability* as opposed to *translational instabilities* which are associated with a purely real eigenvalue of the corresponding linearized system and with eigenvectors localized at the solitary wave.

Frequently, the stability of solitary wave solutions is tested by numerical simulations, i.e., numerically integrating the PDE's with initial conditions corresponding to the solitary wave with possibly some perturbation. While this method is suitable for the identification of strong instabilities and to follow up the evolution of the instability over longer time scales, it may *not* be reliable in general for several reasons. First, weak instabilities may reveal themselves only after very long integration times. If the initial perturbation of the solitary wave solution has no overlap with the eigenvectors associated with the weak instabilities, they would have to evolve essentially out of numerical noise, and may be concealed by numerical instabilities. This applies in principle to any nonlinear system that supports solitary waves. Second, the large spatial extension associated with oscillatory instabilities causes a sensitivity of the stability to the boundary conditions applied to the spatial domain in the numerical simulations. For example, if periodic boundary conditions are applied, there may be a strong sensitivity to the periodicity. As the spatial extension of the eigenvector of an oscillatory instability usually increases with a decreasing growth rate, it is particularly difficult to locate boundaries of stability in parameter space by means of numerical simulations. Third, numerical studies of the spectrum of non-Hermitian eigenvalue problems obtained by linearizing the PDE's around the solitary wave solutions have found spurious eigenvalues, with finite growth rates and associated eigenvec-

tors that strongly oscillate in space. Such spurious eigenvalues occur in large numbers in a treatment of the non-Hermitian operator that is based on a discretization of the spatial domain, and corresponds to finite-difference schemes of numerical simulations [16]. They occur to a lesser but still appreciable extent in a treatment that is still based on real-space discretization but treats the spatial derivatives in Fourier space, thus parallelling beam propagation codes based on the split-step method [16], and they are also present in a scheme that works entirely in Fourier space [7]. These findings imply that such spurious *numerical instabilities* can also occur in numerical simulations of the time evolution of gap solitary waves, and may then mask physical instabilities or false instability, when the solutions are actually stable. The presence of second derivatives in the evolution equations largely suppresses such spurious instabilities. A major goal of this paper is to caution the reader about the use of numerical simulations for the search of instabilities in gap-soliton bearing systems.

The paper is organized in the following way. In Sec. II, our numerical scheme is described in some detail. Although it was already explained in Ref. [16] for the example of gap solitary waves in systems with resonant coupling between fundamental zone-boundary modes and their second harmonics, we feel that it would be in the interest of completeness and reproducibility to give additional details. We also illustrate the aforementioned effect of the sensitivity of the growth rates of oscillatory instabilities with respect to the spatial domain size (the periodicity in the case of periodic boundary conditions) for the example of stationary solitary wave solutions of the MT equations.

Recently Champneys *et al.* [18] considered an extended version of the MT equations that contains second spatial derivatives. These additional terms remove the gap in the linear spectrum of the system. However, these authors were able to find stationary solitary wave solutions. The stability of several examples of such solitary waves is investigated in Sec. III. Furthermore, we introduce additional second-derivative terms that again open a gap in the linear spectrum, albeit with a complicated structure. For this system, a family of multihump solutions is found. It is shown that, depending on a parameter that does not influence the shape of the solitary wave, the time evolution of the latter is dominated either by translational or oscillatory instability.

In Sec. IV, our numerical scheme is applied to the three coupled PDE's studied by Mak *et al.* [17] in connection with gap solitary waves in the presence of second-order nonlinearity under conditions of three-wave mixing. Here it is used for a precise determination of the boundaries of stability. A short discussion ends the paper.

II. NUMERICAL METHOD

The evolution equations considered in this paper are of the general form

$$i\frac{\partial}{\partial\tau}u_\sigma = N_\sigma[u_1,\ldots,u_S], \tag{2.1}$$

where σ runs from 1 to S, $u_1,\ldots,u_S$ are complex functions of time τ and a spatial coordinate ξ, and $N_1,\ldots,N_S$ are nonlinear functions of u_σ, $\sigma=1,\ldots,S$, and their spatial derivatives. Let $u_\sigma^{(s)}(\xi,\tau)=U_\sigma(\xi)\exp(-i\omega_\sigma\tau)$ be a stationary solitary wave solution of Eq. (2.1). Inserting

$$u_\sigma(\xi,\tau)=[U_\sigma(\xi)+a_\sigma(\xi,\tau)]e^{-i\omega_\sigma\tau} \tag{2.2}$$

into Eq. (2.1) and linearizing with respect to the small perturbation a_σ, one is led to a system of linear equations of the form

$$i\frac{\partial}{\partial\tau}a_\sigma(\xi,\tau)=\sum_{\sigma'=1}^{S}[M^{(1)}_{\sigma\sigma'}(\xi)a_{\sigma'}(\xi,\tau)+M^{(2)}_{\sigma\sigma'}(\xi)a^*_{\sigma'}(\xi,\tau)], \tag{2.3}$$

where $M^{(j)}_{\sigma\sigma'}(\xi)$, $j=1$ and 2 and $\sigma,\sigma'=1,\ldots,S$, are linear operators, and a^* is the complex conjugate of a. Defining the $2S$-component vector

$$\mathbf{p}(\xi,\tau)=[a'_1(\xi,\tau),\ldots,a'_S(\xi,\tau),a''_1(\xi,\tau),\ldots,a''_S(\xi,\tau)], \tag{2.4}$$

where a' and a'' are the real and imaginary parts of a, respectively, Eq. (2.3) can be cast into the form

$$\frac{\partial}{\partial\tau}\mathbf{p}(\xi,\tau)=\underline{\mathbf{L}}(\xi)\mathbf{p}(\xi,\tau), \tag{2.5}$$

where $\underline{\mathbf{L}}$ is a real linear matrix operator. Consequently, we may seek complex solutions $\mathbf{p}$ of Eq. (2.5), and construct real solutions by combining $\mathbf{p}+\mathbf{p}^*$ and $i(\mathbf{p}-\mathbf{p}^*)$. Inserting $\mathbf{p}(\xi,\tau)=\mathbf{q}(\xi)\exp(\lambda\tau)$ into Eq. (2.5), one obtains the non-Hermitian eigenvalue problem $\lambda\mathbf{q}=\underline{\mathbf{L}}\mathbf{q}$, which we solve numerically by discretizing the spatial variable ξ, choosing equidistant grid points $\xi_n=n\Delta\xi$, where $n=0,\pm1,\pm2,\ldots,+N$. The spatial derivatives are treated in two alternative ways: The first consists of replacing $\partial q(\xi)/\partial\xi$ at gridpoint $\xi=\xi_n$ by

$$\{q(\xi_{n+1})-q(\xi_{n-1})\}/(2\Delta\xi), \tag{2.6}$$

and likewise $\partial^2 q(\xi)/\partial\xi^2$ by

$$\{q(\xi_{n+1})+q(\xi_{n-1})-2q(\xi_n)\}/\Delta\xi^2. \tag{2.7}$$

This simple discretization allows for the implementation of various boundary conditions at the edges of the spatial domain $\pm L=\pm N\Delta\xi$. The second way of treating the spatial derivatives only applies to periodic boundary conditions. Here the derivative is carried out in Fourier space. This corresponds to replacing $\partial^j q(\xi)/\partial\xi^j$ at gridpoint $\xi=\xi_n$ by the expression

$$\sum_{m=-N+1}^{N}D^{(j)}_{nm}q(\xi_m), \tag{2.8}$$

with

$$D^{(1)}_{mn}=\frac{\pi}{2N\Delta\xi}\begin{cases} i & \text{for } m=n \\ (-1)^{m-n}\left[i-\dfrac{\sin(\pi(m-n)/N)}{1-\cos(\pi(m-n)/N)}\right] & \text{for } m\neq n, \end{cases} \tag{2.9a}$$

$$D^{(2)}_{mn}=-\left(\frac{\pi}{N\Delta\xi}\right)^2\begin{cases} \dfrac{1}{6}(2N^2+1) & \text{for } m=n \\ (-1)^{m-n}\left[\dfrac{1}{1-\cos(\pi(m-n)/N)}\right] & \text{for } m\neq n. \end{cases} \tag{2.9b}$$

This treatment of the spatial derivatives is analogous to that in semispectral integration schemes. It has been found that this second approach considerably reduces the number of spurious eigenvalues as compared to the first one.

In this way, a matrix eigenvalue problem is obtained. The eigenvalues and eigenvectors of the corresponding non-Hermitian matrix are determined by standard diagonalization routines. In the systems we are considering, the spectrum of eigenvalues has the following property: If $\lambda=\lambda'+i\lambda''$ is an eigenvalue of $\underline{\mathbf{L}}$, so are $\lambda'-i\lambda''$ and $-\lambda'\pm i\lambda''$. In the following, we only consider those eigenvalues that have nonnegative real and imaginary parts.

The eigenvectors associated with oscillatory instabilities usually have a spatial extension that strongly exceeds that of the solitary wave itself. With a decreasing growth rate, their spatial width increases. Consequently, it is very difficult to determine accurately the growth rates of weak oscillatory instabilities with the type of calculation described above that works with a finite length $2L$ of the spatial domain. This is illustrated by two examples of stationary solitary wave solutions of the MT equations

$$i\left(\frac{\partial u_+}{\partial\tau}+\frac{\partial u_+}{\partial\xi}\right)+u_-+[N_1|u_+|^2+N_2|u_-|^2]u_+=0, \tag{2.10a}$$

$$i\left(\frac{\partial u_-}{\partial\tau}-\frac{\partial u_-}{\partial\xi}\right)+u_++[N_1|u_-|^2+N_2|u_+|^2]u_-=0, \tag{2.10b}$$

where N_1 and N_2 are constant coefficients and ξ and τ dimensionless variables. Solitary wave solutions of these equations are known analytically [4,5]. A detailed analysis of the stability of stationary and moving solitary solutions of these equations was recently given by Barashenkov and coworkers [20,7] .

In Fig. 1, the dependence of eigenvalues associated with oscillatory instabilities on the length L is shown. For comparison, the spatial extension of the solitary wave is also displayed. Since the separation $\Delta\xi$ between neighboring gridpoints has to be sufficiently small to resolve the spatial variations of the solitary wave and the eigenvectors, the length L is limited by the maximally tractable matrix size in the numerical diagonalization. While eigenvalues with comparatively large growth rates converge at values of L that can be treated with reasonable numerical effort, this is not the case for eigenvalues with smaller growth rates. The growth rates λ' show in fact strong oscillations as functions of L. In the case of Fig. 1(c), the branch of eigenvalues that appears to be the most unstable one at a range of $L=9.5$, where the solitary wave solution has already decayed to almost zero, no longer plays this role at $L=12$; even for this large range, it is not yet clear which branch is the one that has the maximal growth rate.

To cope with this problem, we apply and extend an approach which was devised earlier for a discrete system [24]. It takes advantage of the fact that at distances far from the location of the solitary wave, the operator $\underline{\mathbf{L}}$ is independent of ξ, and its eigenvectors are linear combinations of the form

$$\mathbf{q}(\xi)=\sum_{j=1}^{J} c_j e^{ik_j(\lambda)\xi}\mathbf{w}_j(\lambda)=:\underline{\mathbf{W}}(\lambda,\xi)(c_j)_{j=1}^{J}, \tag{2.11}$$

involving wave numbers k_j which are the roots of the polynomial $\det[\underline{\tilde{\mathbf{L}}}(k)-\lambda\underline{\mathbf{1}}]$, and J is the degree of this polynomial. $\underline{\tilde{\mathbf{L}}}(k)$ is obtained from the operator $\underline{\mathbf{L}}$ by taking the latter at distances $\xi\to\infty$, and replacing an nth spatial derivative by $(ik)^n$. The vectors $\mathbf{w}_j$ are normalized solutions of the linear homogeneous equations

$$[\underline{\tilde{\mathbf{L}}}(k_j)-\lambda\underline{\mathbf{1}}]\mathbf{w}_j=0. \tag{2.12}$$

For a given $\mathbf{q}$, the coefficients c_j may be determined from Eq. (2.11) at gridpoint ξ_N. In case of $J=2S$ as in the MT equations (2.10), $\underline{\mathbf{W}}$ is quadratic. Hence

$$\begin{aligned}\mathbf{q}(\xi_{N+1})&=\underline{\mathbf{W}}(\lambda,\xi_N)\,\mathrm{diag}(\sigma_j e^{ik(\lambda)\Delta\xi})_{j=1}^{2S}(c_j)_{j=1}^{2S}\\ &=\underline{\mathbf{W}}(\lambda,\xi_N)\,\mathrm{diag}(\sigma_j e^{ik(\lambda)\Delta\xi})_{j=1}^{2S}\underline{\mathbf{W}}(\lambda,\xi_N)^{-1}\mathbf{q}(\xi_N),\end{aligned} \tag{2.13}$$

where, in general, $\sigma_j=1$. However, in order to suppress exponentially increasing partial waves in the iterative scheme we put $\sigma_j=0$ for $k_j(\lambda)''<0$. In systems with second order spatial derivatives, $J>2S$. Here, we simply omit the terms with $k_j(\lambda)''<0$ in Eq. (2.11) and, once again, $\underline{\mathbf{W}}$ is quadratic and we may apply Eq. (2.13) as described. For higher derivatives, the coefficients c_j have to be computed from Eq. (2.11), also involving $\mathbf{q}(\xi_n)$ for $n<N$.

Expression (2.13) may be inserted into Eqs. (2.6) and (2.7), giving the derivatives at gridpoint ξ_N in dependence on λ, $\mathbf{q}(\xi_{N-1})$, and $\mathbf{q}(\xi_N)$, but not on $\mathbf{q}(\xi_{N+1})$. The derivatives at gridpoint ξ_{-N+1} are treated in the same way. By this

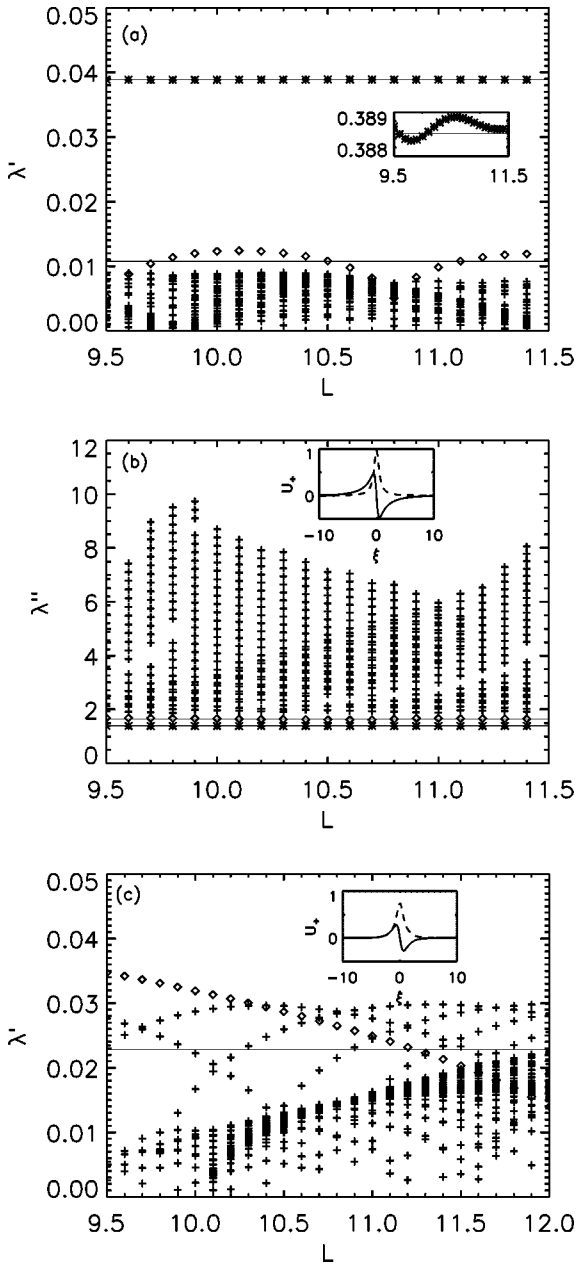

FIG. 1. Dependence of the eigenvalues $\lambda=\lambda'+i\lambda''$ associated with an oscillatory instability on the domain size L. MT equations (2.10) with $N_1=1$ and $N_2=0$. $\omega=-0.9$ [(a) and (b)] and $\omega=-0.1$ (c). Inlays in (b) and (c): real (solid) and imaginary (dashed) parts of U_+. Branches of eigenvalues that are dominant at $L=10$ are shown as diamonds or crosses. The corresponding values for $L=\infty$ are indicated by thin solid lines.

method, one is led to an eigenvalue problem for a matrix $\underline{\mathcal{L}}$ of dimension $4SN\times 4SN$, depending explicitly on the eigenvalue λ,

$$[\underline{\mathcal{L}}(\lambda)-\lambda\underline{1}]\mathbf{q}=0, \tag{2.14}$$

where $\mathbf{q}$ now stands for a $4SN$-component vector.

A determination in this manner of all eigenvalues associated with an instability would require a search of all routes in the complex plane of the secular equation following from Eq. (2.14). This would go beyond our numerical capacities. Instead, we use this approach to accurately determine certain eigenvalues corresponding to the dominant instabilities. We do this by inverse iteration, as described in Ref. [25], starting with initial guesses of λ_0 for the eigenvalue and $\mathbf{q}_0$ for the eigenvector, where $\mathbf{q}_0^*\cdot\mathbf{q}_0=1$. The initial guess is usually motivated by the results of calculations for a large but finite spatial domain size. In the μth step of the iteration, the eigenvalue is updated according to

$$\lambda_{\mu+1}=\lambda_\mu+\frac{\sigma}{\mathbf{q}_\mu^*\cdot\mathbf{v}_{\mu+1}}, \tag{2.15}$$

where $\sigma=1$, and $\mathbf{v}_{\mu+1}$ satisfies

$$[\underline{\mathcal{L}}(\lambda_\mu)-\lambda_\mu\underline{1}]\mathbf{v}_{\mu+1}=\mathbf{q}_\mu. \tag{2.16}$$

The vector $\mathbf{q}_{\mu+1}$ is then defined as $\mathbf{q}_{\mu+1}=\mathbf{v}_{\mu+1}/\sqrt{\mathbf{v}_{\mu+1}^*\cdot\mathbf{v}_{\mu+1}}$.

In the case of diagonalizable matrices that are independent of λ, this procedure converges quickly. The reason, as explained in Ref. [25], is easily seen when expressing $\mathbf{v}_{\mu+1}$ and $q_\mu=\Sigma_n\alpha_n\mathbf{a}_n$ as a linear combination of the normalized eigenvectors of $\underline{\mathcal{L}}$. If λ_μ is close to the eigenvalue $\tilde{\lambda}_0$ of $\underline{\mathcal{L}}$ and sufficiently distant from the other eigenvalues $\tilde{\lambda}_n$, $n\neq 0$, then

$$\mathbf{v}_{\mu+1}=\sum_n\frac{\alpha_n}{\tilde{\lambda}_n-\lambda_\mu}\mathbf{a}_n\approx\frac{\alpha_0}{\tilde{\lambda}_0-\lambda_\mu}\mathbf{a}_0. \tag{2.17}$$

However, if $\underline{\mathcal{L}}$ is dependent on the eigenvalue, a convergence of the procedure is not guaranteed. It deteriorates as the corresponding eigenvalue moves close to other eigenvalues of the matrix. To improve convergence, it is often favorable to vary the initial guess for the eigenvalue and eigenvector and to modify the update of the eigenvalue by choosing the parameter σ in Eq. (2.15) to be smaller than 1. Further statements on the convergence of the procedure in the case of $\underline{\mathcal{L}}$ depending on λ are made in Appendix A. Eigenvalues determined in this way for solitary waves of the MT equations, being of the form

$$u_\pm(\xi,\tau)=U_\pm(\xi)\exp(-i\omega\tau), \tag{2.18a}$$

with

$$U_+(\xi)=U_-^*(\xi)=U(\xi), \tag{2.18b}$$

are shown in Fig. 1 as horizontal lines.

III. HIGHER-ORDER DISPERSION TERMS IN THE MT EQUATIONS

In a recent work, Champneys *et al.* [18] analyzed an extension of MT equations which differ from Eq. (2.10) by the additional term $D\partial^2u_+/\partial\xi^2$ on the left-hand side of Eq. (2.10a) and $D\partial^2u_-/\partial\xi^2$ on the left-hand side of Eq. (2.10b). This addition removes the gap in the linear dispersion relation of Eq. (2.10) (Fig. 2). However, the authors were able to show by numerical analysis that stationary single solitary wave solutions of the form of Eq. (2.18) exist on certain curves in the ω-D plane. Once a stationary solution $U(\xi;\omega,N_1,N_2,D)$ is found, a solution $U(\xi;\omega,N_1',N_2',D)$

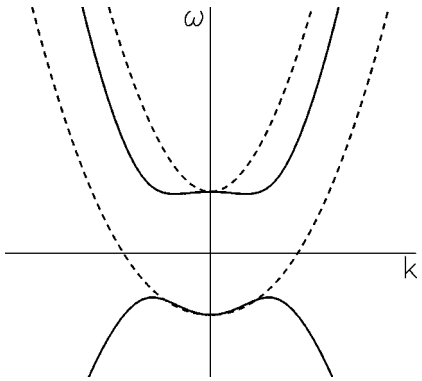

FIG. 2. Linear dispersion relation corresponding to Eq. (3.1). Dashed line: $D=1$ and $\Lambda=0$. Solid line: $D=1/4$ and $\Lambda=1$.

for the same values of ω and D but different values of the constants in front of the nonlinear terms may be obtained by a simple rescaling. This also applies to the stationary solutions of Eq. (3.1) below.

The three stationary single solitary wave solutions given in Figs. 3(a)–3(c) of Ref. [18] are found to be unstable by our numerical stability analysis for different values of N_1. (In the whole of this section, $N_2=1$.) The eigenvalues corresponding to the dominant instabilities are given in Table I.

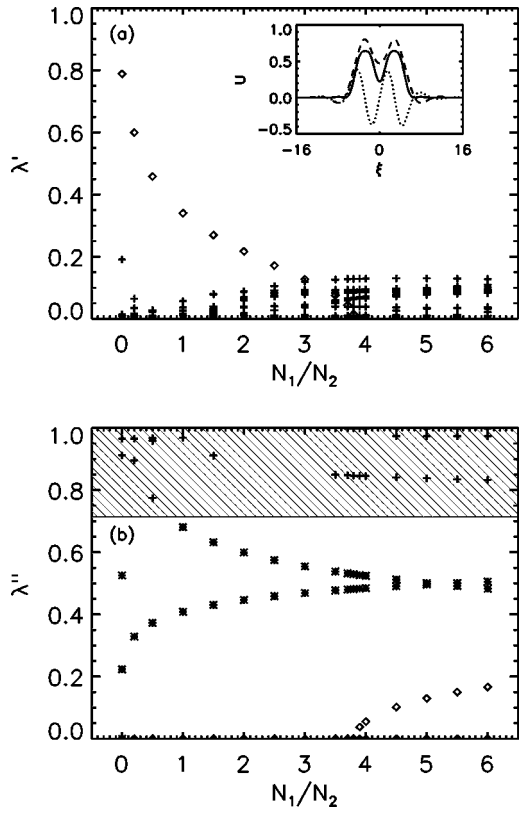

FIG. 3. Dependence on N_1/N_2 of certain eigenvalues $\lambda=\lambda'+i\lambda''$ occurring in the linear stability analysis of a multihump solitary wave solution of Eq. (3.1). $D=1/4$, $\Lambda=1$, and $\omega=0$. We show translational instability (diamonds), oscillatory instabilities (crosses), and internal modes (stars). Hatched area: continuous spectrum of $\underline{\mathbf{L}}$. The inset shows the intensity (solid line) and the real (dashed line) and imaginary (dotted line) parts of the solitary wave U at $N_1=1$ and $N_2=0$.

TABLE I. Eigenvalues corresponding to instabilities with maximal growth rates for the solitary wave solutions given in Fig. 3 of Ref. [18].

D	N_1	λ'	λ''
1.34759 [a]	0.0	1.96	0.0
	1.0	0.53	1.75
	6.0	1.01	2.77
0.53350 [a]	0.0	1.91	0.0
	1.0	0.50	2.60
	6.0	0.95	4.06
0.30595 [a]	0.0	1.96	0.0
	1.0	0.48	3.34
	6.0	1.18	4.46

[a]Values given in Ref. [18]. Frequency $\omega=-0.8$, $N_2=1$.

Because of the fairly large growth rates, it was possible to determine these eigenvalues in calculations for a finite spatial domain and periodic boundary conditions. Special attention has to be paid to the fact that in this system, eigenvectors associated with purely real eigenvalues can still have a large spatial extension because of the absence of a gap in the linear spectrum. This has in fact been observed in the case of small growth rates.

When considering the evolution equations (2.10), with or without an additional second-derivative term, one has to bear in mind that their linear part correctly describes the dispersion relation of the linear excitations in the underlying periodic physical system only for wave vectors near the edges of the Brillouin zone. For small values of the parameter $|D|$, the wave vector of the radiation coupling resonantly to a solitary wave becomes large and, with decreasing $|D|$, one leaves the regime of the validity of the envelope approximation which is the basis for Eq. (2.10). A possibility to avoid such problems and keep the gap open even at large wave vectors is to add further correction terms to the left-hand sides of Eq. (2.10), for example by considering terms that lead to the following equations:

$$i\left(\frac{\partial u_+}{\partial\tau}+\frac{\partial u_+}{\partial\xi}\right)+u_-+[N_1|u_+|^2+N_2|u_-|^2]u_+ +D\frac{\partial^2 u_+}{\partial\xi^2}+\Lambda\frac{\partial^2 u_-}{\partial\xi^2}=0, \tag{3.1a}$$

$$i\left(\frac{\partial u_-}{\partial\tau}-\frac{\partial u_-}{\partial\xi}\right)+u_++[N_1|u_-|^2+N_2|u_+|^2]u_- +D\frac{\partial^2 u_-}{\partial\xi^2}+\Lambda^*\frac{\partial^2 u_+}{\partial\xi^2}=0. \tag{3.1b}$$

The additional terms involving the complex parameter Λ are motivated in the Appendixes for an extension of the original Mills-Trullinger system, where, however, this coefficient would be too small to open the gap, and for the continuum treatment of the diatomic chain. They preserve the conserva-

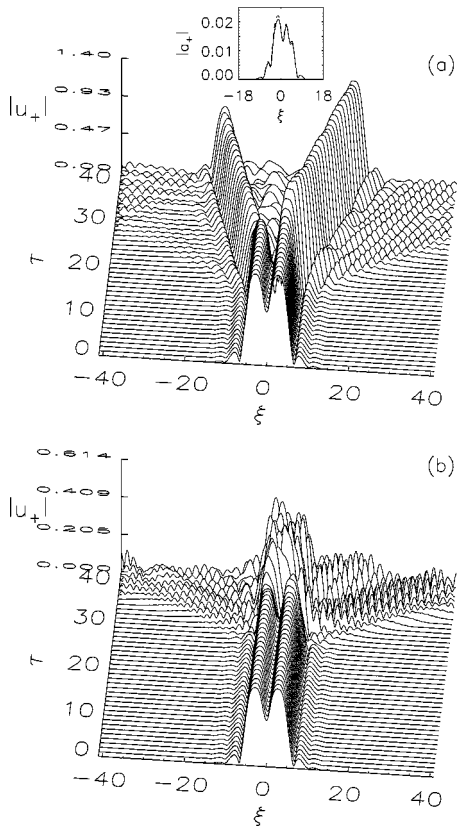

FIG. 4. Time evolution of the multihump stationary solitary wave of Fig. 3. $N_1=0$ (a) and $N_1=6$ (b). Inlay: $|u_+(\xi,10) - U(\xi)|$ (solid line) and $[(a'_+(\xi))^2+(a''_+(\xi))^2]^{1/2}$ (dashed line), where a'_+ and a''_+ are components of the real eigenvector of $\underline{\mathbf{L}}$ corresponding to the translational instability.

tion laws of the MT equations. In particular, the ansatz (2.18) reduces Eqs. (3.1) to ordinary differential equations that have a first integral [see Eq. (B5)].

In the following, we choose Λ to be real for convenience in the numerical calculations. The linear dispersion relation for the system of equations (3.1) is shown in Fig. 2. For fixed values of the parameters in Eqs. (3.1), a one-parameter family of gap solitary wave solutions of the form of Eq. (2.18) is found. As an example, the solution with frequency $\omega=0$ is shown in Fig. 3 (inlay). It exhibits a multihump structure. When analyzing the stability of this solution as a function of N_1 for fixed $N_2=1$, it was found to be always unstable, but the character of its instability changes strongly as N_1 is varied. For small values of $|N_1|$, a translational instability dominates with a growth rate amounting to ≈ 0.8 at $N_1=0$, which dramatically increases as N_1 becomes negative. At $N_1 \approx 3.8$, the translational instability terminates and, in addition to three internal modes, an oscillatory instability remains, though with a very small growth rate. Consequently, solitary wave solutions of Eqs. (3.1) having the same functional form exhibit completely different instability scenarios for different values of N_1. This has been verified in numerical simulations (Fig. 4). The translational instability leads to a splitting of the initial multihump pulse shape, accompanied by a considerable amount of radiation. In contrast to this behavior, the oscillatory instabilities lead to a decay of the solitary wave into short-wavelength fluctuations. In these simulations, the instabilities were not seeded, but developed out of numerical noise.

Both the growth rate and the eigenvector of the instability have been precisely identified in simulations for the case of the translational instability [see the inlay of Fig. 4(a)]. This has been possible to a less satisfactory extent in the case of oscillatory instability, because of the presence of several complex eigenvalues in close vicinity to each other, and because of the fact that simulations can only be done for a finite spatial range. Nevertheless, the growth rate of the dominant oscillatory instability was identified over a certain time interval.

For very small values of Λ and D, chosen such that there is still a gap in the spectrum of linear excitations [$\Lambda=0.3$, $D=0.0$ (i); $\Lambda=0.3$, $D=0.01$ (ii); and $\Lambda=0.3$, $D=0.1$ (iii)], single-hump solitary wave solutions have been found having shapes very similar to that of the Mills-Trullinger solutions. The other parameters in Eqs. (2.18) and (3.1) have been chosen, $\omega=0.5$, $N_2=1$, and $N_1=0$, in order to be close to the integrable case. In the numerical stability analysis applied to solutions as described in Sec. II for several finite ranges L and periodic boundary conditions, no eigenvalues λ with nonzero real parts have been found in case (i) except spurious ones which are associated with the discretization. In cases (ii) and (iii), eigenvalues with very small real parts $|\lambda'|<0.02$ occur with λ' depending on L in a somewhat random fashion. This behavior also occurs in analogous investigations of the MT equations in a parameter region where the solitary waves are supposed to be stable. Therefore, we expect the three solutions (i)–(iii) to be actually stable.

In addition to the above linear stability analysis of single-hump solutions of Eqs. (3.1) which are close to the MT solitary waves, numerical simulations have been carried out on the evolution equations (3.1) with initial conditions at $\tau=0$ corresponding to a pulse solution with $\Lambda=D=0$ to monitor the evolution of MT solitary waves exposed to the influence of small second-order derivative terms. The parameters were again $\omega=0.5$, $N_1=0$, and $N_2=1$. In the case $\Lambda=0.3$ and $D=0.1$ (open gap), the pulse largely retains its shape over time intervals of $\tau>200$ after having shed some radiation. For $\Lambda=0$ and $D=0.1$ (closed gap), the pulse splits after comparatively short times ($\tau\approx 20$) in a scenario similar to that of Fig. 4(a). These findings indicate that, in the absence of a gap, the second-derivative term involving the parameter D plays a destabilizing role.

IV. GAP SOLITARY WAVES VIA THREE-WAVE MIXING

Stationary gap solitary waves have also been studied in systems with second-order nonlinearity. Recently, Mak *et al.* [17] considered a three-wave mixing situation described by the following evolution equations:

$$i\left(\frac{\partial u_1}{\partial \tau}+\frac{\partial u_1}{\partial \xi}\right)+u_2+u_3u_2^*=0, \tag{4.1a}$$

$$i\left(\frac{\partial u_2}{\partial \tau}-\frac{\partial u_2}{\partial \xi}\right)+u_1+u_3u_1^*=0, \tag{4.1b}$$

$$2i\frac{\partial u_3}{\partial \tau}-qu_3+D\frac{\partial^2 u_3}{\partial \xi^2}+u_1u_2=0. \tag{4.1c}$$

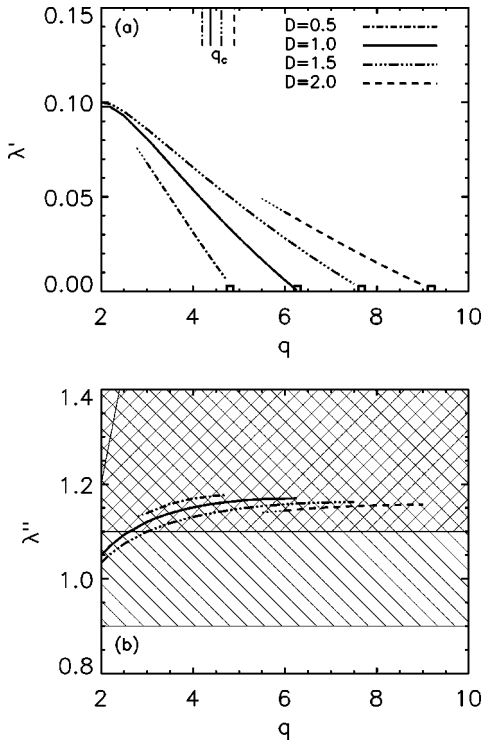

FIG. 5. Dependence of the eigenvalues $\lambda=\lambda'+i\lambda''$ associated with an oscillatory instability on the parameter q for stationary solitary solutions of Eq. (4.1), $k=0.1$. Squares: extrapolated values for q_c. The vertical lines in (a) indicate the values of q_c following from Fig. 4(b) of Ref. [17]. The total hatched region in (b) is part of the continuous spectrum of the operator $\underline{\mathbf{L}}$, and the doubly hatched region is part of the continuous spectrum of the operator $\underline{\mathbf{M}}^{(1)}$ in Eq. (2.3).

In the limit of large q, they reduce to the classical field equations of the massive Thirring model, i.e., the integrable limit of the MT equations [Eq. (2.10), with $N_1=0$].

Stationary solitary wave solutions were obtained via the ansatz $u_\sigma(\xi,\tau)=U_\sigma(\xi)\exp(-i\omega_\sigma\tau)$, $\sigma=1$, 2, and 3, with $U_1=-U_2^*$, U_3 real, and $\omega_3=2\omega_1=2\omega_2$. To follow the notation of Ref. [17], we introduce the parameter k as $k=-\omega_1$. Mak *et al.* checked the stability of these solutions by simulation of their propagation. In this way, they determined boundaries of stability in two-dimensional subspaces of the three-dimensional parameter space.

We have applied the numerical linear stability analysis described in Sec. II to stationary solitary waves on certain lines in the q-D plane of this parameter space. For this purpose, the solitary wave solutions have been recomputed with the help of the shooting method, making use of the fact that the quantity

$$I=2(k+U_3)|U_1|^2+U_1^2+U_1^{*2}+(4k+q)U_3^2-D\left(\frac{\partial U_3}{\partial\xi}\right)^2 \tag{4.2}$$

is independent of ξ.

For those solitary waves that have been found to be unstable, the dominant instability is of oscillatory character. In Fig. 5, eigenvalues $\lambda=\lambda'+i\lambda''$ are shown as functions of the parameter q for four different values of D. The goal of these calculations was to find the values q_c, where the growth rates associated with the oscillatory instability vanish. Therefore, the curves in Fig. 5 have been truncated at an arbitrary point at their left end. The critical values q_c are considerably larger than those following from the stability boundaries given in Fig. 4(b) of Ref. [17] for all four values of D, which illustrates the difficulty of detecting weak oscillatory instabilities in numerical simulations.

In our numerical calculations of the eigenvalues associated with the oscillatory instability, we find that the point of the $\lambda''(q)$ curve, where the growth rate λ' vanishes, is situated inside the continuous spectrum. For the MT equations, Barashenkov *et al.* [20] showed that the oscillatory instability emerges at the point of degeneracy of two internal mode frequencies with a small separation from, but not inside, the continuous spectrum. With our numerical tools, we were not able to identify a mechanism for the creation of an oscillatory instability in the continuous spectrum.

V. CONCLUSION

In summary, a numerical linear stability analysis has been carried out for stationary solitary wave solutions of evolution equations that may be regarded as extensions of the Mills-Trullinger equations describing gap solitary waves in systems with third-order nonlinearity. Higher-order dispersion terms have been introduced into these equations, extending a model considered in Ref. [18] [model (i)], and a model describing a three-wave mixing configuration in a system with second-order nonlinearity discussed in Ref. [17] [model (ii)]. In certain limits of the parameters occurring in these equations, they reduce to the integrable classical field equations of the massive Thirring model.

In model (i), it has been found that by varying the ratio between the two coefficients in front of the nonlinear terms that represent cross-phase and self-phase modulations, the instability scenario of the same multihump solitary wave solution can be strongly changed. In the case of dominant cross-phase modulation, the solitary wave is highly unstable to a splitting into two pulses. When self-phase modulation dominates, oscillatory instabilities with small growth rates remain. In model (ii), boundary points of oscillatory instabilities have been computed on lines in parameter space with a precision that is difficult to achieve in numerical simulations. It has been found that the growth rate associated with the oscillatory instability vanishes at points in parameter space when the corresponding frequency lies in the continuous spectrum of the linearized evolution equations, indicating that the mechanism discovered by Barashenkov *et al.* [20] for the birth of the oscillatory instability in the MT equations does not seem to apply here. It is still an open question what leads to this type of instability in this system.

ACKNOWLEDGMENTS

We would like to thank I. V. Barashenkov, C. Etrich, Yu. S. Kirshar, A. S. Kovalev, and F. Lederer for stimulating discussions. Financial support by the Deutsche Forschungsgemeinschaft (Graduiertenkolleg 176 and Grant No. Ma 1074/6) is gratefully acknowledged.

APPENDIX A: CONVERGENCE PROPERTIES OF THE MODIFIED INVERSE ITERATION PROCEDURE

Assuming that the non-Hermitian matrix $\underline{\mathcal{L}}(\lambda_\mu)$ can be diagonalized at each step μ of the iteration, the following statements concerning the convergence of the iteration can be made. Let λ_* be the correct eigenvalue we want the procedure to converge to, and $\Delta_\mu=\lambda_\mu-\lambda_*$. In addition, we define the vectors $\mathbf{a}_n$, $n=1,\ldots,4SN$, as the right eigenvectors of the matrix $\underline{\mathcal{L}}(\lambda_*)$ normalized according to $\mathbf{a}_n^*\cdot\mathbf{a}_n=1$ and $\mathbf{b}_n^*$, $n=1,\ldots,4SN$, as left eigenvectors of the matrix $\underline{\mathcal{L}}(\lambda_*)$, such that $\mathbf{b}_m^*\cdot\mathbf{a}_n=\delta_{mn}$. $\mathbf{a}_0$ is the right eigenvector and $\mathbf{b}_0^*$ the left eigenvector associated with the eigenvalue λ_*. We also assume that the initial guess for the eigenvalue is already close to λ_* and not close to other eigenvalues of $\underline{\mathcal{L}}(\lambda_*)$. Representing the vectors $\mathbf{q}_\mu$ as linear combinations of the vectors $\mathbf{a}_n$ and $\mathbf{b}_n$, and expanding in powers of Δ_μ, one finds that (i) if $\mathbf{b}_0^*\cdot\mathbf{q}_0$ is not small (i.e., not to first or higher order in Δ_0), then $\mathbf{q}_1=\mathbf{a}_0+O(\Delta_0)$; and (ii) $\Delta_{\mu+1}=(1-\sigma\kappa)\Delta_\mu+O(\Delta_\mu^2)$, where σ is the free parameter in Eq. (2.15), and

$$\kappa=1-\mathbf{b}_0^*\cdot\left[\frac{\partial}{\partial\lambda}\underline{\mathcal{L}}(\lambda)\big|_{\lambda=\lambda_*}\right]\mathbf{a}_0. \tag{A1}$$

From the latter statement we may conclude that for matrices that do not depend on λ, the inverse iteration scheme converges rapidly if σ is chosen to be 1. For values of σ between 1 and 0, the convergence is slower but will still take place. In the case of the matrix $\underline{\mathcal{L}}$ depending on λ, convergence may not be guaranteed if $\kappa\neq1$, even if one starts with an initial guess close to the correct value λ_*. However, it may be achieved by choosing the parameter σ appropriately.

Among the assumptions made to reach statements (i) and (ii), the one concerning sufficient distance of the initial guess from other eigenvalues of $\underline{\mathcal{L}}$ is probably the most difficult to meet in the systems investigated here. Therefore, convergence can be very slow, and the eigenvalues and eigenvectors may undergo considerable jumps from one iteration step to the next.

APPENDIX B: LINEAR CORRECTIONS TO THE MT EQUATIONS

Linear correction terms to the MT equations can be derived in the system originally considered by Mills and Trullinger [4], namely, the propagation of light through a medium with a periodically varying dielectric constant $\varepsilon(z)$. Expanding ε in a Fourier series, keeping only the lowest two Fourier components $\varepsilon(z)=\varepsilon_0+2\varepsilon_1\cos(Gz)+2\varepsilon_2\cos(2Gz+\phi)$, where ϕ is a constant, introducing a stretched coordinate ζ, letting ϵ_1, ϵ_2, and $\partial/\partial\zeta$ be of first order in some expansion parameter η, and expanding to fourth order in η, one finds the following extended version of equations (3.1) of Ref. [4]:

$$\begin{aligned}&[\omega^2-\omega_G^2+O(\eta^2)]E_\pm+\omega^2\frac{\varepsilon_1}{\varepsilon_0}[1+O(\eta)]E_\mp\\&\pm i4\frac{\omega_G^2}{G}[1+O(\eta)]\frac{\partial E_\pm}{\partial\zeta}+\frac{c^2}{\varepsilon_0}[1+O(\eta^2)]\frac{\partial^2E_\pm}{\partial\zeta^2}\\&-2\omega^2\frac{\varepsilon_1\varepsilon_2}{\varepsilon_0}\kappa e^{\pm i\phi}\frac{\partial^2E_\mp}{\partial\zeta^2}+(\text{nonlinear terms})=0,\end{aligned} \tag{B1}$$

where $\kappa=[3(3G/2)^2+\varepsilon_0(\omega/c)^2]/[(3G/2)^2-\varepsilon_0(\omega/c)^2]^3$. Note that there is no first-derivative term $\propto\partial E_\mp/\partial\zeta$, and that the coefficient in front of $\partial^2E_\mp/\partial\zeta^2$ may be complex with a phase factor different from the one in front of $E_\mp$. Due to the factor $\varepsilon_1\varepsilon_2$, the coefficient in front of the second derivative of $E_\mp$ in Eq. (B1) is much smaller than the one in front of the second derivative of $E_\pm$.

This need not be the case in analogous equations arising in the continuum treatment of stationary spatially localized vibrations with frequencies in the phonon gap of a diatomic linear chain. Based on such a continuum approximation, gap solitary waves in diatomic chains with quartic anharmonicity (third-order nonlinearity) were discussed in Refs. [26–28]. We follow and extend these derivations here. In the following, we consider a diatomic chain with harmonic on-site interaction, nearest and second-nearest neighbor intersite interaction, and quartic anharmonic on-site and nearest-neighbor intersite interaction. $u(l,\kappa)$ is the displacement of the particle belonging to sublattice $\kappa=1$ and 2 in the elementary cell l. The particle displacements have to obey the equations of motion

$$\begin{aligned}[M-\Delta M]\ddot{u}(l,1)=&-\phi_1\{2u(l,1)-u(l,2)-u(l-1,2)\}\\&-[\phi_2-\Delta\phi]\{2u(l,1)-u(l+1,1)\\&-u(l-1,1)\}-[K_2-\Delta K]u(l,1)\\&-K_4[u(l,1)]^3-\Phi\{[u(l,1)\\&-u(l,2)]^3+[u(l,1)-u(l-1,2)]^3\},\end{aligned} \tag{B2a}$$

$$\begin{aligned}[M+\Delta M]\ddot{u}(l,2)=&-\phi_1\{2u(l,2)-u(l,1)-u(l+1,1)\}\\&-[\phi_2+\Delta\phi]\{2u(l,2)-u(l+1,2)\\&-u(l-1,2)\}-[K_2+\Delta K]u(l,2)\\&-K_4[u(l,2)]^3-\Phi\{[u(l,2)\\&-u(l+1,1)]^3+[u(l,2)-u(l,1)]^3\}.\end{aligned} \tag{B2b}$$

The deviations, ΔM from the average particle mass and the deviations $\Delta\phi$ and ΔK from the average second-nearest neighbor and on-site force constants are sufficiently small that the linear terms resulting from the deviation from the monatomic chain are of the same order of magnitude as the nonlinear terms. In the latter, we choose the on-site force constant to be the same for the two sublattices.

Stationary solutions are sought with the ansatz

$$u(l,\kappa;t)=(-1)^l e^{-i\omega t}A_\kappa(x(l))+\text{c.c.}, \tag{B3}$$

and the rotating wave approximation is used, which corresponds to neglecting higher time harmonics. The frequency ω has to be equal to or close to the frequency ω_0 at the Brillouin zone boundary of the diatomic chain in the absence of nonlinear terms, and $\Delta M,\Delta\phi,\Delta K=0$ [$\omega_0^2=(2\phi_1+4\phi_2+K_2)/M$.] In Eq. (B3), $x(l)$ is the center of mass of the lth elementary cell with its atoms at their rest positions, and we define $a=x(l+1)-x(l)$ as the lattice constant of the chain. One may now let $A_\kappa(x)$ be continuous functions of x, and expand $A_\kappa(x(l\pm1))=A_\kappa(x(l))\pm a\partial A_\kappa(x(l))/\partial x+\cdots$. Defining new variables $U_\pm(x/a)=A_1(x)\pm iA_2(x)$ and combining Eqs. (B2a) and (B2b), we arrive at the following equations up to terms of order $O(a^3,\Delta\phi a^2)$:

$$\Omega U_\pm=\pm i\frac{\partial U_\pm}{\partial\xi}+\lambda U_\mp+D\frac{\partial^2 U_\pm}{\partial\xi^2}+(\Lambda'\pm i\Lambda'')\frac{\partial^2 U_\mp}{\partial\xi^2}$$
$$\pm Si\frac{\partial^3 U_\pm}{\partial\xi^3}+[N_1|U_\pm|^2+N_2|U_\mp|^2]U_\pm+N_3U_\mp^2U_\pm^*, \tag{B4}$$

with coefficients

$$\Omega=M(\omega^2-\omega_0^2)/\phi_1,\quad \lambda=[\Delta M\omega^2-4\Delta\phi-\Delta K]/\phi_1,$$
$$D=\phi_2/\phi_1,\quad S=1/6,$$
$$\Lambda'=-\Delta\phi/\phi_1,\quad \Lambda''=1/2,$$
$$N_1=3[\Phi+K_4/4]/\phi_1,\quad N_2=2N_1,$$
$$N_3=3[-\Phi+K_4/4]/\phi_1,$$

and $\xi=x/a$. Derivatives in the nonlinear terms have been neglected. It may be noted that in the special case $K_4=4\Phi$, the additional nonlinear term in Eq. (B4) vanishes. Even in the presence of this term, one may seek stationary solitary wave solutions employing the ansatz $U_+=U_-^*=U$. The complex ODE resulting from Eq. (B4) then has a first integral

$$I=-\Omega|U|^2+\frac{\lambda}{2}(U^2+U^{*2})+D\left|\frac{\partial U}{\partial\xi}\right|^2+\frac{1}{2}\left[\Lambda^*\left(\frac{\partial U}{\partial\xi}\right)^2+\Lambda\left(\frac{\partial U^*}{\partial\xi}\right)^2\right]+iS\left[\frac{\partial U^*}{\partial\xi}\frac{\partial^2 U}{\partial\xi^2}-\frac{\partial U}{\partial\xi}\frac{\partial^2 U^*}{\partial\xi^2}\right]$$
$$+\frac{1}{2}(N_1+N_2)|U|^4+\frac{1}{4}N_3[U^{*4}+U^4]. \tag{B5}$$

It should also be noted that Eq. (B4), like Eq. (B1), does not contain a first derivative cross term, i.e., a term $\propto\partial U_\pm/\partial\xi$. If there were such a term, the reduction $U_+=U_-^*$ would no longer give rise to a first integral of the form of Eq. (B5).

[1] B. J. Eggleton, R. E. Slusher, C. M. de Sterke, P. A. Krug, and J. E. Sipe, Phys. Rev. Lett. **76**, 1627 (1996).
[2] E. Yablonovitch, T. J. Gmitter, and K. M. Leung, Phys. Rev. Lett. **67**, 2295 (1991).
[3] N. Aközbek and S. John, Phys. Rev. E **57**, 2287 (1998).
[4] D. L. Mills and S. E. Trullinger, Phys. Rev. B **36**, 947 (1987).
[5] A. B. Aceves and S. Wabnitz, Phys. Lett. A **141**, 37 (1989).
[6] D. N. Christodoulides and R. I. Joseph, Phys. Rev. Lett. **62**, 1746 (1989).
[7] I. V. Barashenkov and E. V. Zemlyanaya (unpublished).
[8] W. E. Thirring, Ann. Phys. (N.Y.) **3**, 91 (1958).
[9] E. A. Kuznetsov and A. V. Mikhailov, Theor. Mat. Phys. **30**, 303 (1977) [Theor. Math. Phys. **30**, 193 (1977)]; D. J. Kaup and A. C. Newell, Lett. Nuovo Cimento Soc. Ital. Fis. **20**, 325 (1977).
[10] C. Conti, S. Trillo, and G. Assanto, Phys. Rev. Lett. **78**, 2341 (1997).
[11] C. Conti, S. Trillo, and G. Assanto, Opt. Lett. **22**, 445 (1997).
[12] H. He and P. D. Drummond, Phys. Rev. Lett. **78**, 4311 (1997).
[13] C. Conti, G. Assanto, and S. Trillo, Opt. Lett. **22**, 1350 (1997).
[14] T. Peschel, U. Peschel, F. Lederer, and B. A. Malomed, Phys. Rev. E **55**, 4730 (1997).
[15] C. Conti, S. Trillo, and G. Assanto, Phys. Rev. E **57**, R1251 (1998).
[16] J. Schöllmann, R. Scheibenzuber, A. S. Kovalev, A. P. Mayer, and A. A. Maradudin, Phys. Rev. E **59**, 4618 (1999).
[17] W. C. K. Mak, B. A. Malomed, and P. L. Chu, Phys. Rev. E **58**, 6708 (1998).
[18] A. R. Champneys, B. A. Malomed, and M. J. Friedman, Phys. Rev. Lett. **80**, 4169 (1998).
[19] T. Iizuka and Yu. S. Kivshar, Phys. Rev. E **59**, 7148 (1999).
[20] I. V. Barashenkov, D. E. Pelinovsky, and E. V. Zemlyanaya, Phys. Rev. Lett. **80**, 5117 (1998).
[21] A. De Rossi, C. Conti, and S. Trillo, Phys. Rev. Lett. **81**, 85 (1998).
[22] I. V. Barashenkov, M. M. Bogdan, and T. Zhanlav, in *Nonlinear World: IV International Workshop on Nonlinear and Turbulent Processes in Physics, Kiev, 1989*, edited by V. G. Bar'yakhtar *et al.* (World Scientific, Singapore, 1990), Vol. 1, p. 3.
[23] I. V. Barashenkov, M. M. Bogdan, and V. I. Korobov, Europhys. Lett. **15**, 113 (1991).
[24] D. Bonart, A. P. Mayer, and U. Schröder, Phys. Rev. B **51**, 13 739 (1995).
[25] W. H. Press, B. P. Flannery, S. A. Teukolsky, and W. T. Vetterling, *Numerical Recipes* (Cambridge University Press, Cambridge, England, 1986).
[26] Yu. S. Kivshar and N. Flytzanis, Phys. Rev. A **46**, 7972 (1992).
[27] C. M. de Sterke, Phys. Rev. E **48**, 4136 (1993).
[28] O. A. Chubykalo, A. S. Kovalev, and O. V. Usatenko, Phys. Rev. B **47**, 3153 (1993).